# Photosensitive Liquid-Crystalline Supramolecules Self-Assembled from Ionic Liquid Crystal and Polyelectrolyte for Laser-Induced Optical Anisotropy

**ARTICLE** *in* MACROMOLECULES · MAY 2008

Impact Factor: 5.8 · DOI: 10.1021/ma800059x



**4 AUTHORS**, INCLUDING:

Xuemin Lu
Shanghai Jiao Tong University
**56** PUBLICATIONS **447** CITATIONS
SEE PROFILE

Qinghua Lu
Shanghai Jiao Tong University
**128** PUBLICATIONS **2,667** CITATIONS
SEE PROFILE

Macromolecules



Article

# Photosensitive Liquid-Crystalline Supramolecules Self-Assembled from Ionic Liquid Crystal and Polyelectrolyte for Laser-Induced Optical Anisotropy

Sufang Xiao, Xuemin Lu, Qinghua Lu, and Bin Su

*Macromolecules*, **2008**, 41 (11), 3884-3892 • DOI: 10.1021/ma800059x • Publication Date (Web): 13 May 2008



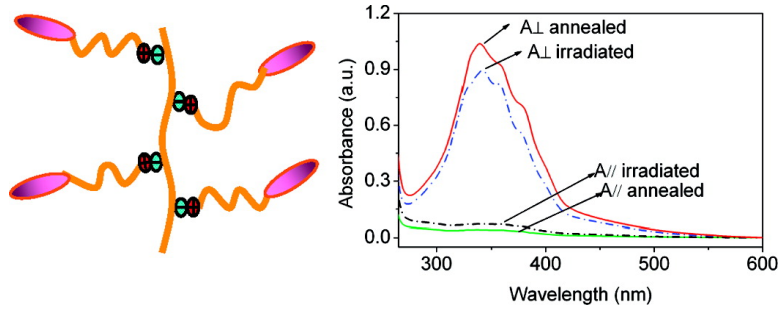


## More About This Article

Additional resources and features associated with this article are available within the HTML version:

- Supporting Information
- Access to high resolution figures
- Links to articles and content related to this article
- Copyright permission to reproduce figures and/or text from this article

View the Full Text HTML

# Photosensitive Liquid-Crystalline Supramolecules Self-Assembled from Ionic Liquid Crystal and Polyelectrolyte for Laser-Induced Optical Anisotropy

**Sufang Xiao, Xuemin Lu, Qinghua Lu,* and Bin Su**

*School of Chemistry and Chemical Technology, Shanghai Jiao Tong University, Shanghai 200240, P. R. China*

*Received January 9, 2008; Revised Manuscript Received March 25, 2008*

ABSTRACT: A new type of thermotropic liquid-crystalline photosensitive supramolecule was fabricated by ionic self-assembly of polyelectrolyte and functional unit azobenzene ionic liquid crystal (azo-ILC). It was found that the thermal and phase behaviors can be modulated by changing of the spacer length (4, 6, or 12 methylene units designated $PAZO_4$, $PAZO_6$, and $PAZO_{12}$, respectively). Highly ordered liquid-crystalline structure with a lamellar morphology of different *d*-spacing was observed. The photoinduced orientation of azobenzene groups in thin films of the obtained ionic-bonding supramolecules was studied by polarized UV−vis and FTIR. Under the irradiation of pulsed laser, very effective induction of optical anisotropy with the preferred direction perpendicular to the pulsed polarization was observed. Typically, the maximum in-plane orientation order (*S*) of −0.93 for $PAZO_{12}$ at maximum absorbance was achieved after irradiation and subsequent anneal at its liquid-crystalline temperature. It was found that the maximum *S* can be increased by increasing the clearing temperature of the photosensitive material. These results may provide guidelines for the design of effective photoinduced anisotropic materials. Furthermore, uniform alignment control of low-molecular-weight liquid crystals on the oriented supramolecular films was achieved.

## Introduction

The generation of anisotropy in films of photosensitive materials, as a fundamental research aspect of materials science and optical technologies, has received much attention because of its applications in information storage, optical processing, holographic grating, liquid crystal alignment, and so on.[1–8] Among photoactive moieties, azobenzene and its analogues are unique photoresponsive systems that are able to display *E*/*Z* isomerization and undergo a photoinduced orientation under polarized light. Presently, various photoresponsive systems including covalent azobenzene polymers,[2–4] polymer matrix doped with azobenzene dyes[5,6] and azobenzene supramolecules[7,8] have been exploited. Among them, azobenzene liquid-crystalline polymer (LCP) was especially concerned due to its reorientation character and pronounced stability of induced optical anisotropy. However, up to now, the maximum in-plane orientation order for a covalent azobenzene-containing LCP is restricted by internal order and rarely exceeds −0.8. Actually, for a practical application such as alignment layers for liquid crystal, polarizers, and many others, a larger optical anisotropy is preferred. It is still a challenging task to find an easy, available, and low-cost approach to obtain photosensitive polymer with optimizing orientation properties. Supramolecular chemistry presents a promising situation that may make unique photochemical and photophysical properties easy to tune and manipulate. Recently, the design and synthesis of functional materials through noncovalent chemistry have been extensively explored due to its distinct advantages over covalent strategies, such as facile, tunable, reversible, and self-repairable.[9–11] A wide variety of recognition motifs are employed including hydrogen bonding,[12] coordination binding,[13] acid−base interaction,[14–17] and Coulombic interaction.[18–21] Ionic self-assembly (ISA) mainly employs the Coulombic interaction to bind the oppositely charged tectonic units together, and the complex architectures can be precisely tailored by the selection of constituents according to the desire of different applications. Many fascinating results have been obtained in the constructing of liquid-crystalline supramolecules with well-defined nanostructure including lamellar, columnar hexagonal, tetragonal, and hierarchical phase microdomain by the ISA technique.[21–25] In these studies, different ISA systems were developed; many polyelectrolyte architectures such as linear and hyperbranched polymers as well as dendrimers have been explored as macromolecular templates and complexed with ionic mesogenes. In most cases, standard, commercially available, charged surfactants have been used; however, more elaborate amphiphilic molecules that are able to introduce new functionalities, such as chirality, polymerizable groups, or photoactive groups inside the ionic self-assembled materials, rarely are explored. We have synthesized an azobenzene-containing lyotropic LC supramolecule based on ISA and showed that moderate optical anisotropy could be laser-induced.[8] However, the photo-orientation was restricted by its rigid molecular structure. In this paper, we intend to design a series of azobenzene thermotropic LCP for tunable phase behavior and improved optical orientation.

Ionic liquids have attracted great interest as environment-friendly versatile media for synthesis and extraction. Except for the well-known dialkylimidazolium and its derivatives, a new kind of ionic liquid named ionic liquid crystal is becoming one of the primary frontiers of research,[26,27] which combines the peculiar properties of liquid crystal and ionic liquid. Thus, it has additional function as reaction media, templates, and even the design of supramolecular materials. Here, as tectonic units, a novel ILC with a azobenzene mesogen substituted in the 4,4′-positions by a methoxy tail and a 4-, 6-, or 12-carbon alkoxy spacer with an ammonium group at its tip was specially designed and synthesized. Further, based on the ionic self-assembly, a new class of azobenzene-containing photosensitive supramolecular material was fabricated. The phase behaviors of the resultant supramolecules of variable alkoxy spacer lengths were identified by cross-polarized optical microscopy (POM), differential scanning calorimetry (DSC), and X-ray analysis. Further, the photoinduced orientation of the complex films under the irradiation of single-beam pulsed laser

* Corresponding author: e-mail qhlu@sjtu.edu.cn; Fax +86-21-54747535.

10.1021/ma800059x CCC: $40.75 
Published on Web 05/13/2008

**Scheme 1. Synthetic Pathway of Ionic Liquid Crystal AZO*i* and Chemical Structure of Liquid-Crystalline Polymers from Ionic Self-Assembly**

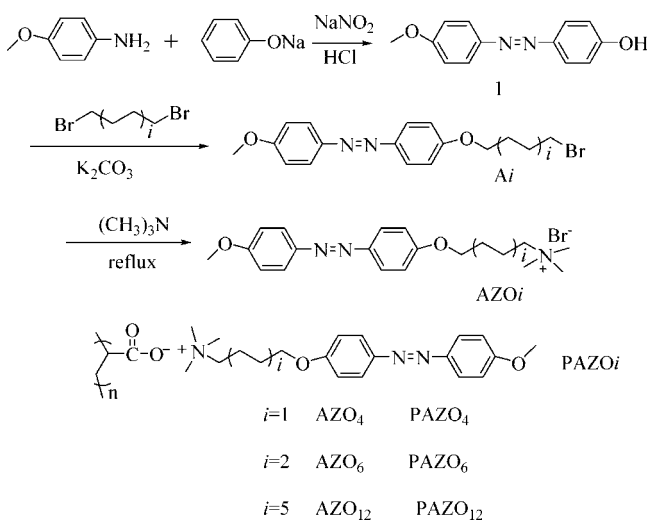


was investigated by polarized UV−vis and FTIR. Our results demonstrated that these photosensitive ionic-bonding supramolecules present a facilely prepared functional material with the capability of undergoing photoinduced generation of prominent optical anisotropy.

## Experimental Section

**Materials and Synthesis.** Poly(acrylic acid) (PAA) 25 wt % solution in water obtained from Alfa Aesar and reported to have a molar mass ($M_w$) of 240 000. Sodium nitrite, phenol, 1,4-dibromobutane, 1,6-dibromohexane, 1,12-dibromododecane, potassium carbonate, 4-methoxyaniline, 33% trimethylamine alcoholic solution, and organic solvents involved in this work were purchased from the Sinopharm Chemical Reagent Co. and used without further purification. The nematic liquid crystal 4-*n*-pentyl-4′-cyanbiphenyl (5CB) was obtained from Slichem LC Materials Co., Shijiazhuang, China. All reagents were of analytical grade. The water used was doubly distilled. Trimethylamine-functionalized azobenzene mesogen with methoxy tail and a 4-, 6-, or 12-carbon alkoxy spacer ($AZO_4$, $AZO_6$, or $AZO_{12}$) was prepared according to Scheme 1. The detailed procedures are described in the following.

*Synthesis of 4-Hydroxy-4′-methoxyazobenzene (***1***).* 4-Methoxyaniline (0.05 mol, 6.16 g) was dissolved in 3 mol/L hydrochloric acid (50 mL). After complete dissolution, the solution was cooled with an ice−salt mixture to a temperature below 5 °C. With vigorous stirring, to this cold solution was added slowly a solution of 3.5 g (0.05 mol) of sodium nitrite in 10 mL of water. The resulting diazonium solution, kept below 5 °C, was subsequently added dropwise to a cold solution of 4.7 g (0.05 mol) of phenol in 25 mL of 10% aqueous sodium hydroxide. The dark brown suspension was acidified, and the precipitate was collected. The crude product was washed with copious amounts of water and dried under vacuum. Yield: 8.6 g, 75%. $^1$H NMR (400 MHz, $CDCl_3$, $\delta$ (ppm)), **1**: 7.86 (ArH, 4H), 7.00 (ArH, 2H), 6.93 (ArH, 2H), 5.25 (OH, 1H), 3.88 ($CH_3O$, 3H).

*Synthesis of 1-Bromo-4-(4-methoxyazobenzene-4′-oxy)butane ($A_1$).* A mixture of **1** (6.85 g, 0.03 mol), 1,4-dibromobutane (13 g, 0.06 mol), potassium carbonate (4.2 g, 0.03 mol), and acetone was refluxed with stirring for 24 h. The reaction mixture was filtered hot, and the residue was washed with acetone. The acetone was removed under reduced pressure and petroleum ether (30−60 °C) was added to the concentrated organic extracts. The resulting precipitate was collected and dried. The crude product was recrystallized with hot filtration from ethanol. Yield: 5.99 g, 58%. $^1$H NMR (400 MHz, $CDCl_3$, $\delta$ (ppm)), $A_1$: 7.87 (ArH, 4H), 7.01−6.96 (ArH, 4H), 3.88 ($CH_3O$, 3H), 4.08 ($OCH_2$, 2H), 3.51 ($CH_2C\mathbf{H}_2Br$, 2H), 2.10−1.98 ($C_2\mathbf{H}_4CH_2Br$, 4H).

*Synthesis of Trimethylammonium-Functionalized 1-Bromo-4-(4-methoxyazobenzene-4′-oxy)butane $AZO_4$.* 3.5 g (0.01 mol) of $A_1$ was dissolved in 25 mL of absolute ethanol. To the warm solution, 5 mL of trimethylamine alcoholic solution 33% was added, and the solution was refluxed for 24 h. Ethanol was removed by evaporation. The crude product was purified by recrystallization from ethanol. $^1$H NMR (400 MHz, DMSO-$d_6$, $\delta$ (ppm)): 7.87 (ArH, 4H), 7.01−6.96 (ArH, 4H), 3.88 ($CH_3O$, 3H), 4.08 ($OCH_2$, 2H), 3.51 ($CH_2C\mathbf{H}_2N$, 2H), 2.10−1.98 ($C_2\mathbf{H}_4CH_2N$,4H), 3.06 ($N(CH_3)_3$, 9H). Trimethylammonium-functionalized 1-bromo-6-(4-methoxyazobenzene-4′-oxy)hexane ($AZO_6$) and trimethylammonium-functionalized 1-bromo-12-(4-methoxyazobenzene-4′-oxy)dodecane ($AZO_{12}$) were synthesized by a similar method. $^1$H NMR (400 MHz, DMSO-$d_6$, $\delta$ (ppm)), $AZO_6$: 7.87 (ArH, 4H), 7.01−6.96 (ArH, 4H), 3.87 ($CH_3O$, 3H), 4.02 ($OCH_2$, 2H), 3.64 ($CH_2C\mathbf{H}_2N$, 2H), 1.82−1.25 ($C_4\mathbf{H}_8CH_2N$,8H), 3.44 ($N(CH_3)_3$, 9H). $AZO_{12}$: 7.81 (ArH, 4H), 7.08−6.84 (ArH, 4H), 3.84 ($CH_3O$, 3H), 4.04 ($OCH_2$, 2H), 3.33 ($CH_2C\mathbf{H}_2N$, 2H), 1.72−1.26 ($C_{10}\mathbf{H}_{20}CH_2N$, 20H), 3.01 ($N(CH_3)_3$, 9H).

**Preparation of ISA Complexes (PAZO*i*).** For the preparation of ISA complex, 10 mg/mL PAA aqueous solution (or sodium polyacrylate aqueous solution obtained from the neutralization of PAA with sodium hydroxide) was added dropwise to AZO*i* aqueous solution with the concentration of 3 mg/mL, in a 1:1 molar charge ratio. The precipitated complex was filtrated and washed several times with doubly distilled water to remove residual salts and possible noncomplexed precursors and then dried in vacuum at 50 °C for 12 h.

**Instruments and Characterization.** FTIR spectra were recorded on a Perkin-Elmer Paragon 1000 FTIR spectrometer on pressed thin transparent disks of the samples mixed with KBr. Spectra were obtained by collecting and averaging 64 scans. Nuclear magnetic resonance ($^1$H NMR) studies were carried out with a Varian Mercury Plus 400 MHz spectrometer in DMSO-$d_6$ or $CD_3Cl$ solvent at room temperature (ca. 25 °C). The chemical shifts were referenced relative to tetramethylsilane. Elemental analysis was performed on a PE 2400 series II of Perkin-Elmer instruments. The samples were dried under vacuum prior to analysis to remove strongly adhering solvent molecules. Thermogravimetric analysis (TGA) was performed using a Perkin-Elmer model 7 instrument. Samples were heated at 20 °C/min from room temperature to 600 °C in a flowing nitrogen atmosphere. Differential scanning calorimetry was performed on a Perkin-Elmer DSC-7 instrument with a 10 °C/min heating rate from −20 to 200 °C under nitrogen. Polarized optical microscopy was performed on a Leica DMLO microscope with a Leitz 350 hot stage. Wide-angle X-ray diffraction (WAXD) was performed on a Bruker-AXS D8 diffractometer (Cu Kα radiation $\lambda = 0.154$ nm, $U = 40$ kV, $I = 100$ mA). Small-angle X-ray scattering (SAXS) experiments were performed using a Bruker Nanostar SAXS instrument at 25 °C. The X-ray source, a 1.5 kW X-ray generator (Kristalloflexn 760) equipped with a Cu tube, was operated at 35 mA and 40 kV. The scattering intensities and patterns were detected by a two-dimensional position-sensitive detector (Bruker AXS) with 512 × 512 channels. The magnitude of scattering vector is given by $q = 4\pi \sin \theta/\lambda$, where $2\theta$ and $\lambda$ are the scattering angle and incident X-ray wavelength (1.542 Å). The distance from sample to detector was 27.1 cm, and the exposure time was 1 h for each sample. The surface morphologies of PAZO*i* films were investigated by atomic force microscopy (AFM, Digital Instruments Inc., Nanoscope IIIa) in contact mode. Absorbance spectra of the PAZO*i* film were recorded using Perkin-Elmer lambda 20 UV−vis spectrophotometer. The polarized FTIR was performed on the Bruker Equinox 55 FTIR spectrometer with a polarizer. The optical anisotropy (degree of molecular orientation) was evaluated by the polarized UV−vis spectra using a Perkin-Elmer lambda 20 UV−vis spectrophotometer equipped with a Glan-Taylor prism.

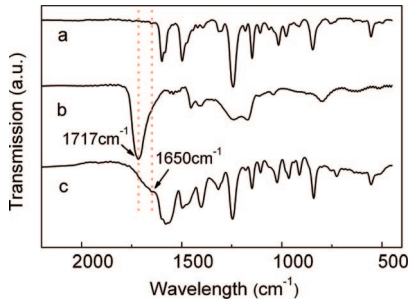


**Figure 1.** FTIR of (a) $AZO_4$, (b) PAA, and (c) $PAZO_4$.

**Laser Irradiation and LC Cell Fabrication.** The PAZO*i* films were prepared by spin-coating a chloroform/ethanol (9/1) solution (30 mg/mL) onto quartz plates, glass slides, and silica substrates (speed: 2000 rpm; time: 20 s). The thickness of the resultant film was about 200−300 nm measured by an ellipsometer.

An s-polarized Nd:YAG laser (355 nm), with a pulse duration of 5 ns and repetition rate of 10 Hz was used as light source. The spin-coated film was fixed on an $X-Y$ platform, and moving speeds were 0.1 and 5 mm/s in $X$ and $Y$ directions, respectively. The incident angle $\theta$ was fixed at 15° with respect to the film normal. The complex films were irradiated at room temperature (about 25 °C) with different exposure fluence.

The photoinduced optical anisotropy in the PAZO*i* film under different irradiation conditions was evaluated by the in-plane order parameter ($S$), which was calculated by[28,29]

$$S = \frac{A_{\parallel} - A_{\perp}}{A_{\text{large}} + 2A_{\text{small}}} \quad (1)$$

$A_{\parallel}$ and $A_{\perp}$ are the absorbance parallel and perpendicular to laser polarization direction (**E**), respectively. $A_{\text{large}}$ and $A_{\text{small}}$ refer to the larger and smaller absorbance of $A_{\parallel}$ and $A_{\perp}$, respectively. Here, $S$ was calculated by polarized UV−vis spectra at maximum absorbance.

A LC cell was fabricated by sandwiching nematic LC (5CB) between a PAZO*i*-coated substrate and a counter buffing polyimide (PI) substrate with the buffing direction parallel to the electric vector E of polarized laser used to irradiate the PAZO*i* film. The two surfaces were separated by 10 $\mu$m spacers and held together using ethoxyline. 5CB was injected to the cell at its isotropic temperature by capillary action. Optical measurements were carried out by placing LC cells between crossed polarizers of POM.

## Results and Discussion

**Synthesis and Characterization of ILC and ISA Complexes.** The preparation of the azo-ILC is outlined in Scheme 1. The $^1$H NMR spectra and assignment of the signals for AZO*i* are depicted in detail in Figure S1. The obtained AZO*i* has considerable solubility in water. The ISA complex as precipitates was obtained by 1:1 charge ratio mixing of two aqueous solutions of AZO*i* and PAA, as described in the Experimental Section. The resultant complexes do not dissolve in water and ethanol, THF, acetone, or nonpolar solvents and only can be dissolved in chloroform/ethanol (v:v 9/1), DMSO, and DMF with excellent solubility. The complexes precipitation has survived multiple washing steps in water, which could selectively remove unbound azo-ILC and PAA. Thus, the successful formation of polymer complexes for AZO*i* with PAA can be testified by FTIR. As an example, the spectra for $AZO_4$, PAA, and their complex $PAZO_4$ are shown in Figure 1. The absorption bands at 1602 and 1500 $cm^{-1}$ in the rigid building units and the complexes are the characteristic peaks of azobenzene. Moreover, the significant shift from 1717 to 1650 $cm^{-1}$ was observed in the C═O vibration band resulting from the complexation between the carboxyl and the ammonium groups,

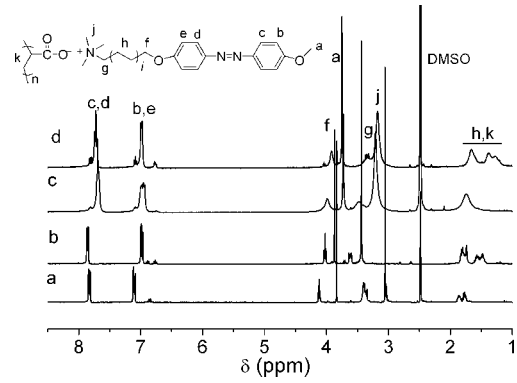


**Figure 2.** $^1$H NMR of (a) $AZO_4$, (b) $AZO_6$, (c) $PAZO_4$, and (d) $PAZO_6$ in DMSO.

which is similar to the assembly of phosphate[25] or alkylcarboxylic acid[17] and polyelectrolyte.

Attempts to support the ionic complexation and establish more accurately the degree of loading, that is, the ratio between carboxylic and ammonium groups, were done by performing NMR and elemental analysis on the complexes. As shown in Figure 2, all proton signals belonging to PAZO*i* and AZO*i* are confirmed and marked clearly. The chemical shifts of 7.87 and 6.98 ppm in PAZO*i* come from the proton signal of the azo-moiety. In complex, the proton signals of the side-chain moiety undergo obviously broadening compared to the resolved resonances of small molecule AZO*i* due to its attachment to PAA. Furthermore, the azo-motif signals of the complex have slight shift to upfield compared to the resource AZO*i*, which result from the influence of the opposite negatively charged main chain. However, the proton signals of PAA were overlapped with that of AZO*i* alkoxy parts. Consequently, it is hardly to estimate the complexation ratio by comparison of the integral of the proton signal of the two buildings. Most insight into the complexes composition came from elemental analysis. As an example, the value for the $PAZO_4$ are given in the following (element: calculated/found) whereby the calculated ones refer to 100% coverage and zero incorporation of bromine. $PAZO_4$: C: 66.7/65.4; H: 7.49/7.81; N: 10.16/9.95; O: 15.47/16.84. These experimental values match the calculated one well; the slight departure may come from the instrument measuring error and minor water, so that a nearly 1:1 ratio complexation of carboxylic and ammonium is indicated. Similarly, for $PAZO_6$ and $PAZO_{12}$, a nearly 1:1 ratio complexation was also confirmed.

**Thermal Analysis and Phase Behavior.** The obtained powder complexes were subjected to thermal analysis to determine their stability and phase behaviors. TGA curves showed that all the complexes are stable up to at least 210 °C (Figure S2), and their thermal stability increase slightly with increasing of their spacer length. The AZO*i* was proved to be thermotropic liquid crystal with reversible phase transition and related characteristics were described in the Supporting Information (Figures S3−S6). The phase behavior of the complexes was investigated in detail by DSC and POM in combination with X-ray analysis; and compared with the tectonic units AZO*i*, absolutely different thermal and phase behavior was observed. As depicted in Figure 3a, the complexes $PAZO_4$ exhibited two clear transition peaks. The first endothermal peak at 67 °C was assigned to the first-order thermodynamic transition. The second broad endothermal peak at 92.2 °C was attributed to the clearing temperature, indicating a transition from a liquid-crystalline phase to an isotropic phase. For $PAZO_6$, the thermal behavior was similar to $PAZO_4$ with a slight lower transition temperature. It is noteworthy that there is a clear hysteresis for the transition

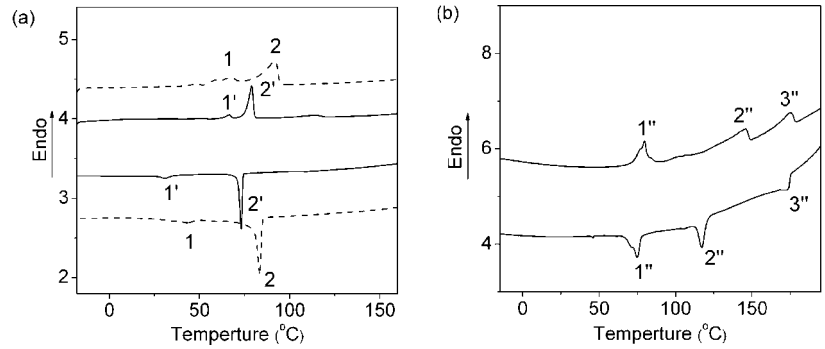


**Figure 3.** DSC curves of (a) $PAZO_4$ (dashed line) and $PAZO_6$ (solid line) and (b) $PAZO_{12}$.

peaks 1 and 1′: on heating, there are some structural changes connected with this transition; on cooling, we observe supercooling and the same structural changes take place. Analogous phenomena have been reported for ionic-bonding supramolecules, and it was attributed to a "stretched-bent shape" transition of the soft alkoxy section accompanied by changes in the packing of the azobenzene units which was connected to the transition of LC phase.[19,30] Surprisingly, compared to $PAZO_4$ and $PAZO_6$, $PAZO_{12}$ presented three reversible transitions with higher transition temperature (Figure 3b). The third endothermal peak at 175 °C corresponded to the transition from a liquid-crystalline phase to an isotropic phase. For the transition peaks 2″ (145.6 °C on heating, 117 °C on cooling), there also is a hysteresis which corresponds to the transition between different phase. Peaks marked with 1″ (79.5 °C on heating, 75 °C on cooling) exhibit excellent reversibility with a symmetrical peak shape, which correspond to the melting and crystallization transition of crystalline alkoxy soft spacer.[14,21,30]

DSC measurements proved that the PAZO*i* complex displays mesomorphic characteristics with temperature variation. The existence of the mesophase was further testified explicitly using POM with hot stage and X-ray analysis. As the complexes and azo-ILC powders were slowly heated from room temperature to 200 °C and then slowly cooled back down to room temperature, different textures were reversibly observed. In the case of $PAZO_4$ and $PAZO_6$, during cooling from isotropic phase, many spherulitic textures with a typical Maltese extinction cross were dispersed in the matrix (Figure 4a,c), which corresponded to the typical nematic droplet and indicated the presence of the thermotropic nematic-type liquid-crystalline state. A typical Schlieren-like texture was observed at 30 °C during cooling process. Here, a smectic phase presenting was preferred to suppose as covalent azobenzene polymer, and more convincing evidence would be provide by X-ray data. For $PAZO_{12}$, a fanlike texture was observed at 170 °C, and it changed corresponding to the transition of the DSC curves during the temperature decrease (Figure 4e−g). However, the observed textures are not the characteristic textures to identify the phase. In order to put more insight into the phase present in the complex materials, X-ray analysis was performed. As shown in Figure 5a, $PAZO_4$ has a reflection peak $q$ at $2\theta = 3.0°$ corresponding to a $d$-spacing of 2.9 nm and a second-order reflection $2q$ at $2\theta = 6.0°$, suggesting lamellar organization of smectic structure. For $PAZO_6$, the two reflections at $2\theta = 1.96°$ and $2\theta = 2.56°$, marked with $q_1'$ and $q_1$, along with well-defined $2q_1'$ ($2\theta = 3.94°$), $3q_1'$ ($2\theta = 5.92°$), $2q_1$ ($2\theta = 5.22°$), and $3q_1$ ($2\theta = 7.88°$), indicating the coexistence of two-scale-size lamellar nanostructures with a periodicity of 4.5 and 3.4 nm, respectively. We proposed that the two sizes of lamellar organization are related to the packing of soft section of the complex and the stacking of rigid azobenzene part.[31] As shown in Figure 5b, in the case of $PAZO_{12}$ at 25 °C, a lamellar phase with $d$-spacing of 3.6 nm ($2\theta = 2.45°$) is easily identified (marked with $q_2$). The more clear reflection at even lower $2\theta$ angles, marked with $q_2'$, along with a faint reflection $2q_2'$, is indicative of a relatively disordered lamellar superstructure with a $d$-spacing 6.0 nm within the material. In accordance with the DSC analysis, the in-situ temperature-dependent X-ray data showed that, only when the temperature is lower than the crystallization temperature, the reflections $q_2'$ and $2q_2'$ appear, indicating that the superstructure is connected to the crystallization of the soft section of the complex. It is noteworthy that the reflections $q_2$, $2q_2$, and $3q_2$ remain unchanged during the cooling. We presumed that the ordered lamellar structure was from the organization of rigid azobenzene and frozen during cooling. In Figure 5c, wide-angle profiles show a broad peak at wide angle around 20° and several sharp peaks indicating that the crystalline exists in the complexes. It appears that, with the increasing of the segregation between the azobenzene and polymer backbone, the degree of crystallization of the complexes increased. Especially $PAZO_{12}$, it is a typical crystalline supramolecular polymer, which is in good agreement with its long alkoxy molecular structure and supported above assignment to its phase nanostructure. According to the above results, the phase sequence and transition temperature are summarized in Table 1.

**Orientation of Azobenzene Groups in PAZO*i* Film under Pulsed Irradiation.** The spin-coated PAZO*i* films were proved to be isotropic and uniform with low surface roughness by optical microscopy and AFM. Results from the UV−vis spectroscopic investigation of the resultant complexes, as a typical example, $PAZO_4$ in solution or film, are presented in Figure 6. For the sample in solution, the small shoulder at ~460 nm is assigned to $n-\pi^*$ transition and the maximum of the absorbance in the range of 340−360 nm corresponds to a strong $\pi-\pi^*$ electronic transition of *E*-isomer of the azo-moiety.[4] Maxima of the absorbances of the $PAZO_4$ complexes in chloroform/ethanol (v:v 9/1)) and film are at 355 and 318 nm, respectively. The dramatic blue shift of the maximum of the azobenzene chromophores in film compared with that of solution implied the existence of aggregates.[18]

The *E*/*Z* isomerization of azobenzene groups occurs upon actinic irradiation. Compared to linear UV light or continued laser, the irradiation by pulsed laser not only induces *E*/*Z* isomerization and photo-orientation of azobenzene groups in PAZO*i* film but also involves the possibility of fast thermal heating. In this work, an s-polarized pulsed laser (355 nm) was used as light source.

It was widely reported that thermal annealing at liquid-crystalline phase led to an enhancement of the orientation of liquid-crystalline polymer films.[32,33] The photoinduced orientation behaviors as well as the influence of thermal treating for the irradiated films were investigated. Here, annealing at 80 °C for 10 min for the irradiated $PAZO_4$ film and 120 °C for 10 min for the irradiated $PAZO_{12}$ were adopted as the thermal treating conditions. Figure 7a shows the changes in the

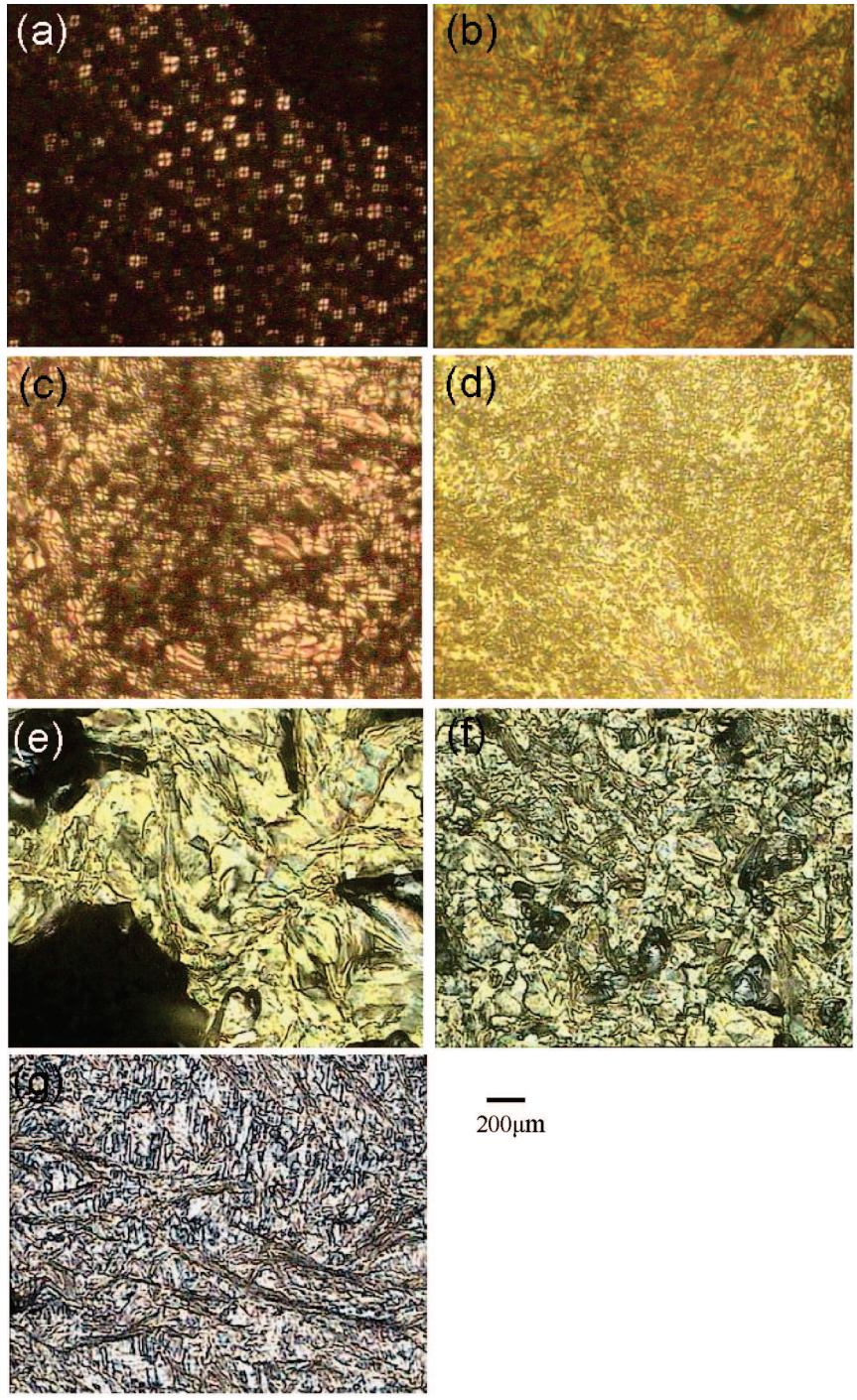


**Figure 4.** Typical polarized optical micrographs of the texture of $PAZO_4$ at (a) 80 °C and (b) 30 °C, $PAZO_6$ at (c) 70 °C and (d) 30 °C, and $PAZO_{12}$ at (e) 170 °C, (f) 100 °C, and (g) 30 °C during cooling from their isotropic phase.

polarization UV−vis spectra of $PAZO_4$ film irradiated with 3.0 mJ/cm$^2$ of polarized laser and after subsequent annealing. After irradiation, the absorbance in the direction perpendicular to laser polarization, $A_\perp$, is obviously larger than the absorbance parallel to laser polarization, $A_\parallel$, which indicated that the preferred direction of the azobenzene chromophores is perpendicular to the laser polarization direction. The annealing enhances the optical anisotropy due to its LCP nature. In this case, the in-plane orientational order $S$ at 315 nm is amplified from −0.39 to −0.53, and the negative sign of in-plane orientation order means that the photoinduced orientation is perpendicular to the polarization of the pulsed laser. $PAZO_6$ presented similar photo-orientation behaviors which are consistent with their similar molecular structure and thermal properties. For $PAZO_{12}$, as shown in Figure 7b, after irradiation with 10.0 mJ/cm$^2$, a much larger optical anisotropy with in-plane order $S$ −0.89 at 340 nm was induced. After annealing, the in-plane order $S$ increased to −0.93, which is the reported crowning value. The photo-orientation of covalent azo-dendrimer by the same light source as present system has been studied deeply in our group, and the maximum $S$ of −0.45 was obtained after irradiation and subsequent annealing.[4] In another typical system, the maximum $S$ of −0.80 for covalent azobenzene side-chain polymer was obtained by exposing to nonpolarized 365 nm light followed by irradiating with linear polarized 633 nm and annealing.[29] We should note that the maximum in-plane order for an azobenzene-containing polymer is usually in the range from −0.2 to −0.8.[18] The pronounced induced optical anisotropy in

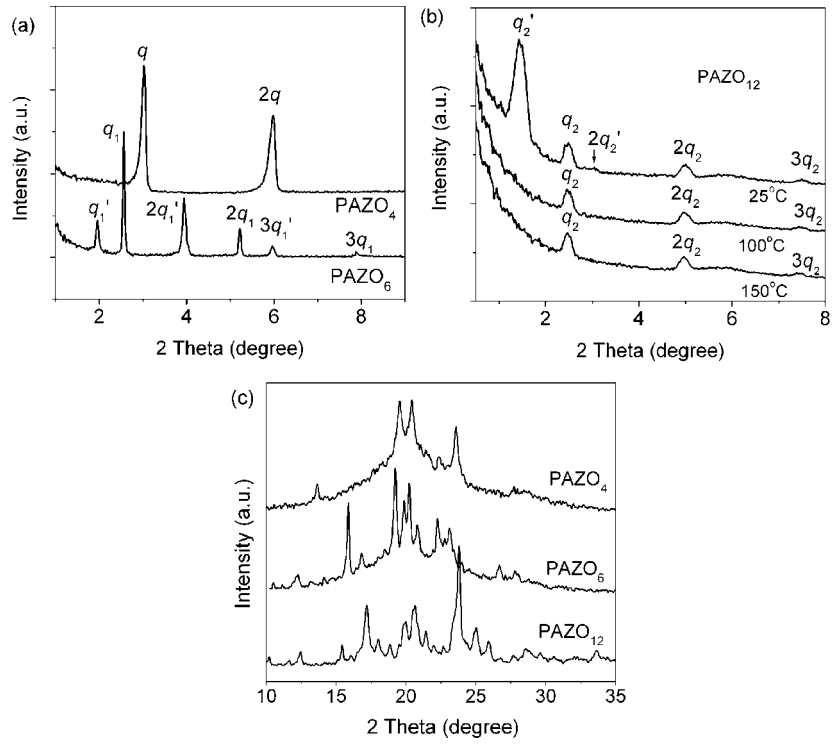


**Figure 5.** (a) SAXS profiles of complex of $PAZO_4$ and $PAZO_6$ at room temperature after annealed from their isotropic phases, (b) SAXS profiles of $PAZO_{12}$ at different temperature during cooling from isotropic phases, and (c) WAXD profiles of complex of $PAZO_4$, $PAZO_6$, and $PAZO_{12}$ at room temperature after annealed from their isotropic phases.

**Table 1. Assignment of Phases of the Complexes**

| | thermal transition (°C) | |
|---|---|---|
| complexes | heating | cooling |
| $PAZO_4$ | S (Sm) 67.0 N 92.2 I | S (Sm) 44 N 83.2 I |
| $PAZO_6$ | S (Sm) 66.6 N79 I | S (Sm) 32 N 73 I |
| $PAZO_{12}$ | S (Cr 79) 146 Sm 175 I | S (Cr 75) 117 Sm 173 I |

[a] I = isotropic phase; N = nematic phase; Sm = smectic phase; S = solid state; Cr = crystalline phase. Transition temperatures are the peak temperature of DSC profiles.

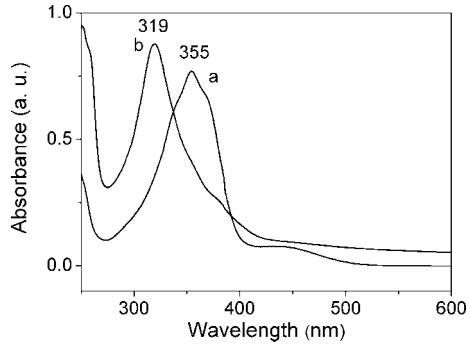


**Figure 6.** Normalized UV−vis spectra of (a) $PAZO_4$ in chloroform/ethanol (9:1, ca. $10^{-7}$ mol/L) and (b) $PAZO_4$ film.

this work may come from its high transition temperature and the typical ionic-bonding LC polymer nature. For any practical application, the time and temperature stability of the orientated anisotropic surface are particularly important. The orientation stability was tested by keeping the orientated films at room temperature for 2 months, and negligible decrease of *S* was observed. The thermal endurance of the induced anisotropy was tested by annealing the irradiated film at 80−200 °C for 30 min. The dichroic ratio was examined every 5 °C. The results proved that, for $PAZO_4$ at 95 °C and $PAZO_{12}$ at 175 °C, they still preserve about 80% of the maximum of orientation. Compared with that of covalent-bonded polymer, the high density of charge in ionic complex leads to the strong and long-range Coulombic interaction with reduced relaxations and to the high viscosity. This feature of ionic complex makes the orientation very stable even at above its clearing temperature.

The in-plane orientation order of the complex films changed when the exposure energy of laser varied. As depicted in Figure 8a, for $PAZO_4$, the in-plane orientation order of azobenzene groups increases with increasing of laser fluence, and the maximum value of −0.39 is achieved at 3.0 mJ/cm$^2$. Then the orientation order begins to decrease with the increase of laser fluences. A similar relation between *S* and laser fluences was observed for $PAZO_{12}$ (Figure 8b). In contrast, the maximum *S* is achieved at higher exposure fluence 10.0 mJ/cm$^2$ for $PAZO_{12}$. This evolution can be interpreted by the intrinsic character of the pulsed laser. Actually, the pulsed laser induces photo-orientation of azobenzene groups accompanied by fast thermal heating due to nanosecond pulse.[34,35] The strong thermal effects leads to local melting of the film surface, which makes the orientation of azobenzene groups easier and also leads to the relaxation of oriented molecules. At the end of each pulse, the film is solidified and the remained orientation is frozen. That is to say, both laser intensity and surface temperature are the key factors in deciding the final anisotropic orientation of azobenzene groups, and they show contrary effect on the orientation order. At lower laser fluence, thermal effect is rather weak, and the final orientation order increases with the increase of laser fluences. While at higher fluence, the thermal effect becomes strong and leads to the relaxation of oriented molecules.[36,37] The contrary factors of the laser orientation and thermal relaxation result in the above nearly parabola variation of the anisotropic orientation with laser fluence. Accordingly, it is easy to understand that the complex film ($PAZO_{12}$) with a higher transition and clearing temperature consequentially display higher saturation value of *S* at larger laser fluence. This result may provide a guideline for the design of photosensitive materials possessing effective photoinduced anisotropy by pulsed laser.

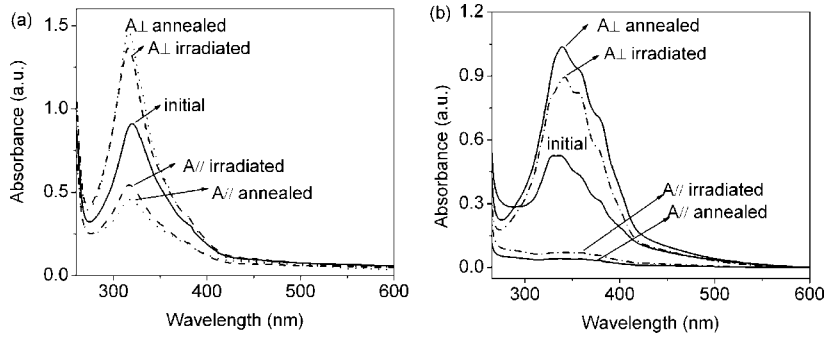


**Figure 7.** Changes of polarized absorbance spectra in the films of (a) $PAZO_4$ irradiation with 3.0 mJ/cm$^2$ and after annealing at 80 °C for 10 min and (b) $PAZO_{12}$ irradiation with 10.0 mJ/cm$^2$ and after annealing at 120 °C for 10 min. $A_{||}$ and $A_{\perp}$ are the absorbance parallel and perpendicular to laser polarization direction (**E**), respectively.

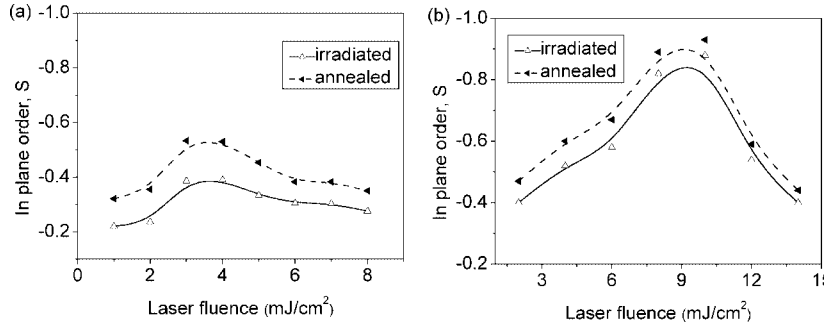


**Figure 8.** In-plane orientation order of (a) $PAZO_4$ (calculated at 315 nm) and (b) $PAZO_{12}$ (calculated at 340 nm) as a function of laser fluences.

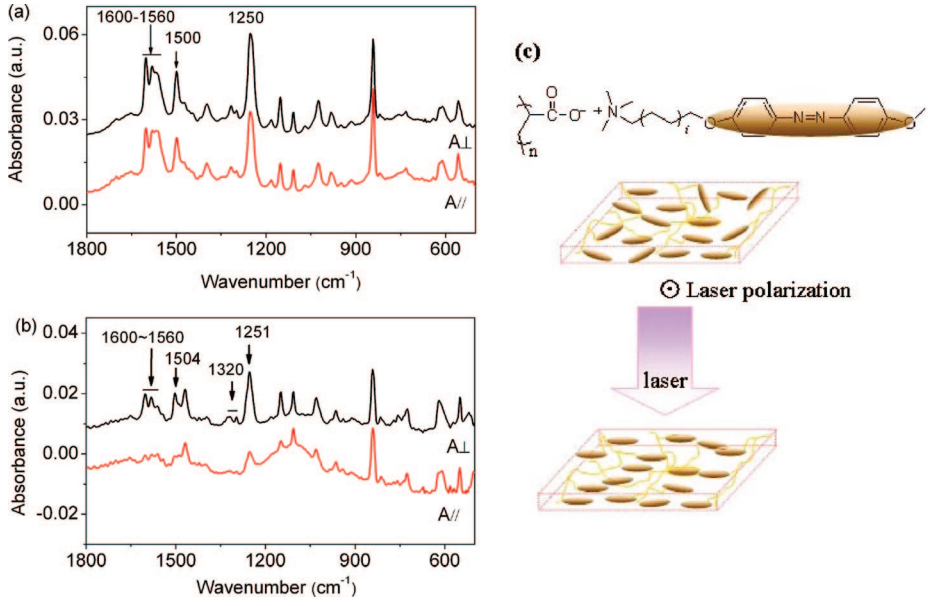


**Figure 9.** Polarization FTIR spectra of irradiated (a) $PAZO_4$ film with the fluence 3.0 mJ/cm$^2$ and (b) $PAZO_{12}$ film with the fluence 8.0 mJ/cm$^2$ on silica substrate and (c) illustration of the photo-orientation of PAZO*i* films.

The molecular reorientation behaviors of the mesogenic side groups are further elucidated by polarization FTIR spectroscopy. Figure 9 shows the polarization FTIR spectra of $PAZO_4$ and $PAZO_{12}$ films spin-coating on silica after irradiation by pulsed laser. A large negative dichroism ($A_{||} - A_{\perp} < 0$) for absorptions 1600−1560, 1500, and 1250 cm$^{-1}$ are observed, which corresponding to the vibration of −C═C of phenyl and −N═N− (usually overlapped with that of phenyl backbone) and Ph−O of phenol. These results supported that the rigid part azobenzene of the side chain aligned with the preferred direction perpendicular to the pulsed polarization. Consistent with the result of polarized UV, $PAZO_{12}$ presents more effective photoinduced anisotropy with a larger dichroism as displayed in Figure 9b. Based on the above results, an orientation scheme proposal was given in Figure 9c, which explicitly describes the photoresponsive processes of PAZO*i* supramolecular films.

**Alignment Behavior of LC on the Irradiated PAZO*i* Films.** In order to prove the potential application of this novel liquid-crystalline supramolecules in device or optical components, preliminary optical investigations in the field of LC alignment were performed. It is well-known that the alignment of LC molecules can be controlled by anisotropic surface of alignment layer, either by its topography or by oriented

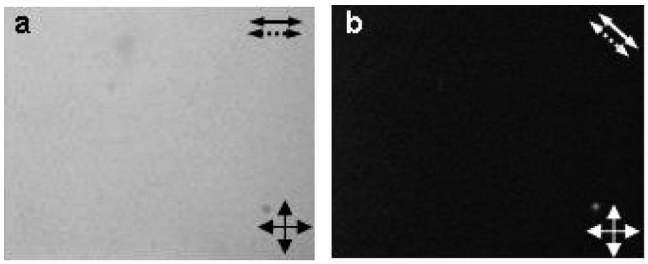


**Figure 10.** POM images of LC alignment on the irradiated $PAZO_4$ (with the fluence 3.0 mJ/cm$^2$) substrate taken between crossed polarizers: (a) the buffing direction parallel to one of the polarizer axes and (b) the buffing direction at 45° to each polarizer axis. The arrows indicate the buffing direction of the counter polyimide substrate (<—> upper plate) and the direction of laser polarization (<•••> lower plate).

molecular chains, which are referred to as "command surfaces". Here, as an example, an oriented $PAZO_4$ film was evaluated as the alignment layer of low-molecular-weight LC 5CB. To investigate the LC alignment on the azobenzene-containing complexes after being irradiated by laser, a LC cell was assembled using the irradiated film of $PAZO_4$ and a PI counter substrate buffed in the direction perpendicular to laser polarization acting on $PAZO_4$, isotropic 5CB was injected into the cell by capillary force and the cell gap was fixed to 10 $\mu$m using a polyethylene film. As a control experiment, the as-spin-coated $PAZO_4$ film and buffed PI was constructed to LC cell with the same technique. The cells were examined by placing LC cell between two crossed polarizers of POM. In the case of the control cell, the Schlieren-like texture of 5CB was observed, which illustrated that the 5CB was in random state, though the buffed PI substrate has the capability to align the LC. For the irradiated $PAZO_4$ cell, as shown in Figure 10, the light field presented alternative change of dark or bright under crossed polarizers according to the rotation of the cell with a period 90°, which illuminated explicitly the homogeneous and stable LC alignment was achieved on the $PAZO_4$ anisotropic orientation film. Additionally, we have also investigated the irradiated $PAZO_6$ and $PAZO_{12}$ films, and in all cases the homogeneous and stable LC alignment was obtained.

## Conclusion

In this contribution, we have proposed a new type of photosensitive thermotropic liquid-crystalline supramolecules and demonstrated pronounced photoinduced orientation. The materials were fabricated by the ionic couple of poly(acrylic acid) and elaborately designed azo-ILC. With the variation of the alkoxy spacer length, highly ordered lamellar liquid-crystalline nanostructure with different *d*-spacing was achieved. More importantly, a prominent photoinduced orientation was obtained by irradiation of the resultant ISA film with pulsed laser. Typically, the maximum $S$ of $-0.93$ for $PAZO_{12}$ at maximum absorbance was obtained after irradiation and subsequent anneal at 120 °C. Polarized UV and FTIR spectroscopies displayed that the preferred direction of the azobenzene chromophores is perpendicular to the laser polarization direction. The anisotropic orientation behavior proved to be changed with the laser fluences in a parabola function, which resulted from the contrary action of the thermal relaxation effect and photoinduced orientation of pulsed laser. It was found that the maximum $S$ can be increased by increasing the transition and clearing temperature of the photosensitive material, which may provide guidelines for the design of effective photoinduced anisotropic materials. Moreover, an oriented PAZO*i* film was evaluated as the alignment layer of low-molecular-weight LC. Uniform LC alignment control with a twist of 90° was obtained in a combined LC cell made up of an oriented PAZO*i* coated substrate and a buffed polyimide. The POM proved that LC molecules aligned along the oriented azobenzene chain of the PAZO*i* surface. All the results approved that the obtained ionic-bonding supramolecular polymer possesses the capability of more effective photoinduced anisotropy than traditional azobenzene polymer with good stability and can be used as photosensitive functional materials in many potential fields. It is anticipated that this line of research may open avenues for the design of functional materials with preferable properties.

**Acknowledgment.** We gratefully acknowledge the support of the National Science Foundation of China (Grant No. 60577049) and the Projects (05JC14019, 0652 nm017) of the Science and Technology Commission of Shanghai Municipal Government.

**Supporting Information Available:** NMR assignments for AZO*i*; TGA curves of the complexes PAZO*i*; DSC, POM, and X-ray profiles of AZO*i*. This material is available free of charge via the Internet at http://pubs.acs.org.

## References and Notes

(1) Natansohn, A.; Rochon, P. *Chem. Rev.* **2002**, *102*, 4139–4175.
(2) Wu, Y.; Demachi, Y.; Tsutsumi, O.; Kanazawa, A.; Shiono, T.; Ikeda, T. *Macromolecules* **1998**, *31*, 349–354.
(3) Sapich, B.; Vix, A.; Rabe, J. P.; Stumpe, J. *Macromolecules* **2005**, *38*, 10480–10486.
(4) Li, X.; Lu, X. M.; Lu, Q. H.; Yan, D. Y. *Macromolecules* **2007**, *40*, 3306–3312.
(5) Gibbons, W. M.; Shannon, P. J.; Sun, S. T.; Swetlin, B. J. *Nature (London)* **1991**, *351*, 49–50.
(6) O'Neill, M.; Kelly, S. M. *J. Phys. D: Appl. Phys.* **2000**, *33*, 67–84.
(7) Gao, J.; He, Y. N.; Liu, F.; Zhang, X.; Wang, Z. Q.; Wang, X. G. *Chem. Mater.* **2007**, *19*, 3877–3811.
(8) Xiao, S. F.; Lu, X. M.; Lu, Q. H. *Macromolecules* **2007**, *40*, 7944–7950.
(9) Faul, C. F. J.; Antonietti, M. *Adv. Mater.* **2003**, *15*, 673–683.
(10) Binnemans, K. *Chem. Rev.* **2005**, *105*, 4148–4204.
(11) Zhou, S.; Chu, B. *Adv. Mater.* **2000**, *12*, 545–556.
(12) Bazuin, C. G.; Brodin, C. *Macromolecules* **2004**, *37*, 9366–9372.
(13) Valkama, S.; Lehtonen, O.; Lappalainen, K.; Kosonen, H.; Castro, P.; Repo, T.; Torkkeli, M.; Serimaa, R.; ten Brinke, G.; Leskelä, M.; Ikkala, O. *Macromol. Rapid Commun.* **2003**, *24*, 556–560.
(14) Zhou, S.; Shi, H.; Zhao, Y.; Jiang, S.; Lu, Y.; Cai, Y.; Wang, D.; Han, C. C.; Xu, D. *Macromol. Rapid Commun.* **2005**, *26*, 226–231.
(15) Bazuin, C. G.; Boivin, J.; Tork, A.; Tremblay, H.; Bravo-Grimaldo, E. *Macromolecules* **2002**, *35*, 6893–6899.
(16) Tork, A.; Bazuin, C. G. *Macromolecules* **2001**, *34*, 7699–7706.
(17) Thünemann, A. F.; General, S. *Langmuir* **2000**, *16*, 9634–9638.
(18) Zakrevskyy, Y.; Stumpe, J.; Faul, C. F. J. *Adv. Mater.* **2006**, *18*, 2133–2136.
(19) Franke, D.; Vos, M.; Antonietti, M.; Sommedijk, N. A. J. M.; Faul, C. F. J. *Chem. Mater.* **2006**, *18*, 1839–1847.
(20) Zakrevskyy, Y.; Faul, C. F. J.; Guan, Y.; Stumpe, J. *Adv. Funct. Mater.* **2004**, *14*, 835–841.
(21) Canilho, N.; Kasëmi, E.; Schlüter, A. D.; Mezzenga, R. *Macromolecules* **2007**, *40*, 2822–2830.
(22) Chen, H.-L.; Lu, J.-S.; Yu, C.-H.; Yeh, C.-L.; Jeng, U.-S.; Chen, W.-C. *Macromolecules* **2007**, *40*, 3271–3276.
(23) Hanski, S.; Houbenov, N.; Ruokolainen, J.; Chondronicola, D.; Iatrou, H.; Hadjichristidis, N.; Ikkala, O. *Biomacromolecules* **2006**, *7*, 3379–3384.
(24) Canilho, N.; Kasëmi, E.; Mezzenga, R.; Schlüter, A. D. *J. Am. Chem. Soc.* **2006**, *128*, 13998–13999.
(25) Ozer, B. H.; Smarsly, B.; Antonietti, M.; Faul, C. F. J. *Soft Matter* **2006**, *2*, 329–336.
(26) Yang, J.; Zhang, Q. H.; Zhu, L. Y.; Zhang, S. G.; Li, J.; Zhang, X. P.; Deng, Y. Q. *Chem. Mater.* **2007**, *19*, 2544–2550.
(27) Chiou, Josh, Y. Z.; Chen, J. N.; Lei, J. S.; Lin, Ivan, J. B. *J. Mater. Chem.* **2006**, *16*, 2972–2977.
(28) Meier, J. G.; Ruhmann, R.; Stumpe, J. *Macromolecules* **2000**, *33*, 843–850.
(29) Uchida, E.; Shiraku, T.; Ono, H.; Kawatsuki, N. *Macromolecules* **2004**, *37*, 5282–5291.

(30) Zakrevskyy, Y.; Stumpe, J.; Smarsly, B.; Faul, C. F. J. *Phys. Rev. E* **2007**, *75*, 031703(1) −031703(12)
(31) Guan, Y.; Antonietti, M.; Faul, C. F. J. *Langmuir* **2002**, *18*, 5939–5945.
(32) Fischer, T.; Läsker, L.; Czapla, S.; Rübner, J.; Stumpe, J. *Mol. Cryst. Liq. Cryst.* **1997**, *297*, 489–496.
(33) Uchida, E.; Kawatsuki, N. *Macromolecules* **2006**, *39*, 9357–9364.
(34) Evans, K. E. J. *Appl. Phys.* **1988**, *63*, 4946–4950.
(35) Bartholomeusz, B. J. *Appl. Opt.* **1992**, *31*, 909–918.
(36) Lu, Q. H.; Wang, Z. G.; Yin, J.; Zhu, Z. K.; Hiraoka, H. *Appl. Phys. Lett.* **2000**, *76*, 1237–1239.
(37) Hildebrandt, R.; Hegelich, M.; Keller, H. M.; Marowsky, G.; Hvilsted, S.; Holme, N. C. R.; Ramanujam, P. S. *Phys. Rev. Lett.* **1998**, *81*, 5548–5551.

MA800059X